

CONF-771015--13

INTERACTION OF A PLANE FLAME FRONT  
WITH THE WAKE OF A CYLINDER\*†

I. Namer<sup>††</sup>, Y. Agrawal, R. K. Cheng,  
F. Robben, R. Schefer, L. Talbot<sup>††</sup>

October 1977

MASTER

Energy and Environment Division  
LAWRENCE BERKELEY LABORATORY

—NOTICE—

This report was prepared as an account of work sponsored by the United States Government. Neither the United States nor the United States Department of Energy, nor any of their employees, nor any of their contractors, subcontractors, or their employees, makes any warranty, express or implied, or assumes any legal liability or responsibility for the accuracy, completeness or usefulness of any information, apparatus, product or process disclosed, or represents that its use would not infringe privately owned rights.

\* To be presented at the Fall Meeting, Western States Section of The Combustion Institute, October 17-18, Stanford, California.

1977

† This work was primarily supported by the Air Force Office of Scientific Research. The experimental equipment and technique were also jointly supported by ERDA, Division of Basic Energy Sciences, and ERDA, Division of Conservation Research and Technology.

†† Also Mechanical Engineering Department, University of California, Berkeley.

## **DISCLAIMER**

**This report was prepared as an account of work sponsored by an agency of the United States Government. Neither the United States Government nor any agency Thereof, nor any of their employees, makes any warranty, express or implied, or assumes any legal liability or responsibility for the accuracy, completeness, or usefulness of any information, apparatus, product, or process disclosed, or represents that its use would not infringe privately owned rights. Reference herein to any specific commercial product, process, or service by trade name, trademark, manufacturer, or otherwise does not necessarily constitute or imply its endorsement, recommendation, or favoring by the United States Government or any agency thereof. The views and opinions of authors expressed herein do not necessarily state or reflect those of the United States Government or any agency thereof.**

## **DISCLAIMER**

**Portions of this document may be illegible in electronic image products. Images are produced from the best available original document.**

## ABSTRACT

A Rayleigh scattering and laser Doppler velocimetry system has been developed for studying the interaction between the vortex street behind a cylinder and a two dimensional plane flame front. Measurements on an open jet methane/air flame stabilized on a heated 0.25 mm platinum wire showed appreciable instabilities in the flame due to the turbulent eddies in the mixing region of the jet. By enclosing the flow in a square channel flame stability was increased. A 3.2 mm diameter cylinder, with  $U_d/v = 90$  and  $f_d/U = 0.16$ , was used to generate a Kármán vortex street at a frequency of 22 Hz. Measurements indicated that the flame motion in the wake is small compared to the scale of vortices shed by the cylinder, but the rms fluctuations in velocity in the wake of the cylinder were comparable to the rms fluctuations in Rayleigh scattering through the flame. Furthermore, the flame upstream of the wake region also fluctuated which would indicate that as a portion of the flame fluctuates, it perturbs the entire flow field upstream.

## INTRODUCTION

The interaction between fluid mechanical turbulence and the combustion process has long been recognized as important to the understanding of combustor performance<sup>(1)</sup>. Numerous turbulent flame speed models have been proposed, but as yet no complete theory exists which satisfactorily accounts for the observed phenomenon<sup>(2)</sup>. This lack of understanding is readily apparent in numerical modeling of turbulent combustion. For example, several recent studies aimed at predicting pollutant formation in turbulent reacting flows using time averaged approaches and simplified turbulence models have met with only fair success, and the principal result from these studies is a recognition of the need for more realistic models<sup>(3,4)</sup>.

This situation is largely due to the lack of reliable experimental data. However, the recent development of Rayleigh scattering and laser Doppler velocimetry for localized density and velocity measurements should make possible the necessary time and space resolution required for a more precise description of turbulence and combustion interactions. Furthermore, the recent recognition of large coherent structures in many turbulent flows<sup>(5)</sup> require their consideration in the turbulent modeling. It was decided to use a simplified experimental model of this sort of turbulence by studying the interaction of a Kármán vortex street with a flame.

The overall objectives of the present investigation are to determine the general characteristics of flame front propagation in a turbulent premixed flow and to develop an understanding of the various interactions which occur between fluid mechanical turbulence and the heat release due

to the combustion process. This report presents the results of preliminary measurements on a free standing flame front stabilized on a hot wire or a small cylinder. The objectives were to determine (a) the stability of the resulting flame front under laminar flow conditions and the source of any instabilities if they do exist, (b) the ability of Rayleigh scattering and laser Doppler velocimetry to provide accurate density and velocity measurements in a flame system, and (c) to investigate the fluctuations in the flame front caused by the Kármán vortex street shed by a cylinder.

Two sets of measurements are described in the following. The first were carried out in a 5 cm diameter open jet with the flame stabilized on a heated platinum wire and measurements of the average flame profiles and fluctuations due to the flow system are reported. The second set of measurements were made in a 5 cm square channel with the flame stabilized in the wake of a small rod. The fluctuations due to the flow system were much smaller and measurements of the flame profile and fluctuations in the wake of a second rod were carried out.

#### EXPERIMENTAL APPARATUS AND PROCEDURE

##### Flow System

A schematic diagram of the experimental apparatus is shown in Fig. 1. A mixture of metered gases (air and methane in any combination) are brought into a stagnation chamber of 20 cm diameter equipped with wire screens to damp out flow turbulence. From this chamber the flow passes either through a 5 cm diameter nozzle to an open jet (Fig. 2) or through a 5 cm square nozzle

into a square channel with pyrex walls, shown in Fig. 3. The stagnation chamber is mounted on an X-Y-Z traverse mechanism so that the optical system can remain stationary. All gases are metered individually using rotameters. The gas mixture can also be seeded with  $Al_2O_3$  particles for laser anemometry measurements. To provide a particle free flow for Rayleigh scattering measurements it was necessary to install an oil/water removal filter and a 1  $\mu m$  particle filter in the house air system. A 30 cm long, 7.5 cm diameter mixing chamber filled with 5 mm glass beads assures thorough premixing of gases.

#### Flame Stabilization

A variety of flame stabilizers have been used by previous investigators<sup>(2,6)</sup>. These include single and multiple rods, wires, disks, wall recesses, vee gutters, and flat plates. Two important considerations in the selection of a suitable stabilizer are the resulting stability characteristics and turbulent disturbances generated by the flame holder itself. Flame stability is enhanced by a large strongly recirculating wake region downstream of the flame holder<sup>(6)</sup>. It is necessary to minimize this latter effect if turbulence levels are to be effectively controlled.

Several stabilizers were tried during the course of this study. In the open jet measurements a 0.25 mm diameter electrically heated platinum wire was used as shown in Fig. 2. The small diameter of the wire minimizes the effect of body generated turbulence on the flame front, and by heating the wire stabilization was possible over a reasonable range of flow conditions. The two plates shown in Fig. 2 functioned as a

chimney and reduced somewhat the turbulent fluctuations in the mixing regions of the jet and the ambient air, which in turn reduced the fluctuations in the flame.

In the closed channel experiments the wake of a 1.6 mm diameter rod was used to stabilize the flame, as some difficulties were encountered with the small platinum wires. There did not appear to be any fluctuations in the flame front due to the wake of this rod.

#### Rayleigh Scattering and LDV Systems

A schematic of the Rayleigh and LDV optics system is shown in Fig. 4. In both cases a 4 watt argon ion laser operating at 488 nm was used. For the LDV measurements, beam splitting is accomplished with a back to back prism arrangement which makes it possible to adjust the beam intersection to the desired point and thus minimize the measurement volume size and achieve a more uniform fringe spacing. Seeding of the flow is accomplished with a particle generator where choked air jets (0.4 mm dia.) skim the surface of a suspension of 3  $\mu\text{m}$  nominal diameter  $\text{Al}_2\text{O}_3$  particles in water. This particle generator is capable of providing a relatively constant particle seeding rate of up to 2000 particles/sec over a period of several hours. Particle sizing was done using an impactor plate separator developed at LBL. The resulting mass ratio of particles less than 2.4  $\mu\text{m}$  to those greater than 2.4  $\mu\text{m}$  was found to be approximately 8.0. Frequency demodulation of the Doppler signal is done by a commercial TSI 1090 LDV tracker.

Measurements of gas density from Rayleigh scattering are carried out using F/1.2 collection optics and an F/6 0.3 m McPherson spectrometer. An uncooled RCA 1P28 photomultiplier tube is used as the detector

with the output read directly on an electrometer. The laser beam is focused by a 100 mm focal length lens to a 70  $\mu\text{m}$  waist diameter. Laser light scattered at a 90° angle is then collimated by an F/1.2 collection lens and refocused on the entrance slit of the spectrometer. The resulting measurement volume is a cylinder 1.0 mm in length by 70  $\mu\text{m}$  in diameter (Fig. 2). References (7), (8), and (9) give a more complete discussion of the theory behind Rayleigh and LDV scattering. The probability density and spectrum of the tracker output are obtained using a Federal Scientific correlator and spectrum analyzer.

### EXPERIMENTAL RESULTS AND DISCUSSION

#### Open Jet Measurements and Discussions

It is well known that laser beam deflection and broadening can result due to gradients in the index of refraction in the flame<sup>(9)</sup>. Since loss of spatial resolution can result, this effect was investigated by imaging the measuring volume onto a screen while at the same time traversing the flame with the laser beam parallel to the flame front. A maximum deflection in the beam of one beam diameter (70  $\mu\text{m}$ ) was observed in a direction normal to the flame front. Several traverses were repeated with the laser beam inclined at a small angle to the flame front. This in effect reduced the length of beam subjected to large density gradients. Negligible improvement in the beam deflection was noted at angles up to 5°. Angles greater than 5° would result in a loss of spatial resolution greater than that due to beam deflection.

Experimental measurements of flame density profiles were carried

out for a methane air flame at an equivalence ratio of 0.755 and a nozzle exit velocity of 1.15 m/s. The corresponding Reynolds' number based on wire diameter was 19.6. The results are shown in Figs. 5, 6, and 7 where normalized Rayleigh scattering intensity and rms fluctuation are plotted against distance from the jet centerline. The Rayleigh scattering intensity is related to the gas density through the following equation<sup>(7)</sup>

$$I_R = CI_0 N \sum X_i \sigma_{Ri} \quad (1)$$

where  $I_R$  is the intensity of Rayleigh scattered light,  $C$  is a calibration constant of the optics,  $I_0$  is the incident laser light intensity,  $N$  is the total molecular number density,  $X_i$  is the mole fraction of the species, and  $\sigma_{Ri}$  is the Rayleigh cross section.  $\sigma_{Ri}$  is related to the index of refraction  $n_i$  by the expression:

$$n_i - 1 = \frac{\lambda_0^2 N_i}{2\pi} \sigma_{Ri}^{1/2}$$

As will be discussed later, the Rayleigh scattering intensity is directly proportional to density and found to be independent of the changes in gas composition during combustion to within 3% accuracy for the present system. Traverses were taken across the flame normal to the free stream flow direction (not normal to the flame front) at distances of 3 mm, 6 mm, and 12 mm downstream of the wire.

Fluctuations in the flame front location were readily apparent. Two forms of instability were present. The first was a low frequency ( $\sim 1$  cps) visibly observable random flame front movement. This is represented by the error bars shown in the data and represents an average uncertainty in

flame front position of 0.1 mm, 0.25 mm, and 1.0 mm for the three cases respectively. This effect could be due to several sources. Velocity profiles were measured using the LDV system above the nozzle to determine flow uniformity in the absence of combustion. These are shown in Fig. 8 along with rms values of velocity fluctuations. Data are presented at distances of 3, 6, and 12 mm above the nozzle exit and it can be seen that the velocity profiles are uniform over the entire region in which Rayleigh measurements were taken. RMS velocity fluctuation values of approximately 2% were measured at the nozzle centerline and these increased to a maximum of 10% at a distance of 24 mm from the centerline. At 7 mm from the centerline (corresponding to the maximum distance over which Rayleigh measurements were taken) the fluctuations have increased to approximately 4%.

The most likely source of the disturbance is the turbulent mixing of the jet with the ambient air, and the resulting interaction with the flame front as it penetrates this turbulent region. When this turbulent mixing zone was greatly minimized in the channel experiments discussed later, the entire flame region could be made quite steady. Apparently these disturbances must propagate back upstream and along the flame front. The presence of the two walls shown in Fig. 3 also reduced the flame fluctuations somewhat.

In addition to the random fluctuations discussed above, flame front oscillations were found to exist at well defined frequencies of 88 and 135 cps. A typical oscilloscope trace of these fluctuations, as well as the corresponding spectrum analysis of this signal, are shown in Fig. 9. RMS values for these oscillations normalized by the local scattering intensity are shown in Figs. 5, 6, and 7. For both the 3 mm and 6 mm cases, a

maximum normalized rms fluctuation of approximately 0.30 was observed.

In the 12 mm case, the maximum rose sharply to 0.62, indicating increased fluctuations as one moves farther downstream.

A comparison between experimentally measured and calculated values of the Rayleigh intensity ratio across the flame was made. The calculated value, based on the assumption of adiabatic combustion with equilibrium products, was found to be 0.153. The corresponding experimental value (from Eq. 1) was  $0.155 \pm 0.01$ , indicating good agreement. The above calculation was repeated assuming 100%  $N_2$  at the adiabatic flame temperature to investigate the effect of mixture composition on the Rayleigh signal. Agreement was within 3% of the value assuming equilibrium products. This indicates that the scattered intensity is approximately independent of the degree of reaction and inversely proportional to the density for the conditions of this experiment.

For an idealized one dimensional flame front inclined at an angle  $\theta$  to the incoming gas flow, the burning velocity  $U_b$  is related to the incoming velocity  $U_i$  by the expression<sup>(6)</sup>

$$U_b = U_i \sin \theta \quad (2)$$

In actual flame systems the flow upstream of the flame front diverges so that Eq. (2) does not hold unless the right hand side is replaced by the component of flow velocity normal to a particular flame front isotherm. Based on measurements taken at 3 mm and 6 mm points, the flame inclination angle was found to be  $22.3^\circ$ . For an incoming velocity of 1.15 m/s, Eq. (2) gives a burning velocity of 0.43 m/s. This compares with a laminar flame speed of 0.26 m/s<sup>(10)</sup> for a  $CH_4$ /air flame at the same conditions.

Smith and Gouldin<sup>(11)</sup> have noted in a similar study using LDV and hot wire anemometry that consideration of flow divergence upstream of the flame front could result in flame speeds lower by up to 50% over those determined by the direct angle method (Eq. (2)) and probably will largely account for the difference in flame speeds.

A comparison of flame front thickness was made with values published in the literature. The apparent flame front thickness was determined from the experimental Rayleigh intensity profiles, Figs. 5 through 7. A conventional definition for flame front thickness was used which is given by<sup>(12)</sup>

$$L = \frac{\rho_b - \rho_u}{(dp/dz)_{\max}} \quad (3)$$

where  $\rho$  is the gas density and the subscripts b and u refer to burned and unburned gases respectively.  $(dp/dz)_{\max}$  is the maximum density gradient in the flame zone. Values calculated from Eq. (3) for the three cases of the present investigation are shown in Table I. These can be compared with a value of 0.96 mm from the literature<sup>(12)</sup>.

TABLE I - Flame Front Thickness

Distance above Flame Holder, mm	Flame Front Thickness, mm
3	0.80 $\pm$ .15
6	1.12 $\pm$ .33
12	1.89 $\pm$ .28

The estimated error limits on the calculated values of this investigation are based on uncertainty in the flame front location due to the random fluctuations noted earlier. It can be seen that the values at 3 mm and 6 mm from the flame holder are comparable with the published value. As one moves downstream, however, the averaged flame front thickness increases significantly. This increase is probably due to fluctuations in flame front position. Under conditions of turbulent upstream flow Smith and Gouldin<sup>(11)</sup> also noted a similar increase in flame front thickness.

The results of LDV measurements across the flame are shown in Fig. 10 for the velocity component parallel to the jet axis. At distances of 3 and 6 mm above the wire a relatively well defined velocity increase of 10% indicates the location of the flame front while at 12 mm downstream the velocity profile has become quite spread out and it is difficult to determine a flame front location. Flame front positions determined from Fig. 10 are in general agreement with those determined from the Rayleigh results. The flame spread angle and flame speed were calculated based on the point at which the velocity had increased by 2% from the free stream value. The resulting flame speed was 0.48 m/sec, compared with a value of 0.43 m/s calculated from Rayleigh scattering measurements. Considering difficulties in defining a flame front location for the two sets of measurements such agreement is reasonable.

RMS values for velocity fluctuations were measured and found to be in the same range as those shown in Fig. 8 for flow above the nozzle without combustion. No oscillations were observed at 88 and 135 cps as was found during the Rayleigh measurements. However, based on flame front fluctuations indicated by the Rayleigh measurements, maximum velocity fluctuations on the order of 3% would be expected due to the relatively small changes in velocity across the flame. Noting that the minimum sensitivity

of the present LDV system appears to be 2 to 3%, it is possible that the fluctuations could be present but below measureable limits.

#### Closed Channel Measurements and Discussion

In order to reduce the fluctuations in the flame front the flow system was changed to 5 cm square channel with pyrex walls, as shown in Fig. 3, and the flame was stabilized in the wake of a 1.6 mm diameter rod. Stephenson<sup>(13)</sup> has found that flame movement along a wall can be minimized by injecting a thin layer of  $N_2$  along the wall to effectively quench the flame in the region. This was done through 100  $\mu m$  porous material, 3.2 mm thick at the base of each of the pyrex walls. The nitrogen also helped keep the flame from flashing back along the corners of the nozzle where the velocity gradients are relatively small. The flow field without combustion was mapped with a hot film anemometer and found to be uniform. Turbulence levels were of the order of 1.5% and lower. The velocity at the channel entrance was 0.424 m/s and the equivalence ratio of the methane/air flame was 0.77.

Rayleigh scattering profiles were taken of the undisturbed flame at distances of 5, 7.5, 10, and 12.5 mm downstream of the flame holder. A typical profile is shown in Fig. 11. The scattering of laser light from the pyrex windows of the channel into the detection optics was a substantial fraction of the signal, ranging from 20% to 100% of the Rayleigh signal from room temperature air. This background scattering was strongly dependent on the dirt and imperfections in the pyrex glass wall where the laser beam entered and exited the channel, and thus would vary strongly from measurement point to measurement point. A correction for the background scattering was made for every measurement by moving the image of

the spectrometer slit to positions just above and below the laser beam, where there is no Rayleigh scattering signal but where the background scattering is approximately the same. These intensities were averaged (they were not equal, in general) and subtracted from the Rayleigh plus background measurement to obtain the Rayleigh scattering. Even this correction procedure had considerable inaccuracy, and is probably responsible for much of the error in the data to be presented. By comparisons, the background scattering was negligible in the open jet flame profile measurements described previously.

It was also found that the Rayleigh signal in the region of the flame front oscillated slowly and somewhat irregularly at a rate of about one cycle every two minutes. Apparently the flame position was varying by as much as 1 mm, even though the flow rate remained steady. We have conjectured that this wandering may be due to some thermal effect associated with the channel walls. In any event the origin has not been determined and it was a source of considerable error.

No indications of fluctuations in the Rayleigh scattering signal in the region of the flame front (or at any position) were found, for frequencies up to approximately 100 Hz. There is, of course, the shot noise generated by the photoelectron collection in the photomultiplier. This noise is independent of frequency and was subtracted from the measured rms fluctuations. The actual sensitivity of the overall system to fluctuations in density was about 1% for frequencies up to 1000 Hz.

The effect of fluctuations in the flow field on the flame front was investigated by allowing the Kármán vortex street behind a cylinder to interact with the flame front. As shown in Fig. 3, a 3.2 mm diameter rod was placed in the same axial location as the flame holder, with 8 mm transverse

separation. According to Kovásznay<sup>(14)</sup>, there is a unique relation between the cylinder Reynolds number and the Strouhal number,  $St = fd/U$ , where  $f$  is the frequency of vortex shedding,  $d$  is the rod diameter, and  $U$  is the free stream flow velocity. There is also a critical Reynolds number of 40 below which there is no Kármán vortex street. The Reynolds number of the 3.2 mm rod was 90, corresponding to a Strouhal number of 0.16 and vortex shedding at 21.2 Hz.

Profiles of the mean Rayleigh scattering signal and the rms fluctuations were taken in the region of the flame at a series of axial positions. Spectral analysis of the fluctuations indicated a peak at 22 Hz, which compares well with the predicted value of 21.2 Hz. There was also an additional peak at 10.5 Hz with about half the amplitude, which is as yet unaccounted for. For the measurements to be reported the rms value of the fluctuations, over a bandpass of approximately 5 Hz to 1000 Hz, was measured with an rms meter while the average values were either read from the electrometer or from a digital voltmeter.

A typical profile of the mean Rayleigh signal where the flame is in the wake of the rod is shown in Fig. 12. The two flame profiles sketched indicate the apparent maximum excursions of the slow 0.5 cycle per minute fluctuation in flame position. One should note that the accuracy of these measurements is limited, due to the uncertain background scattering signal, and that the true flame density profile could have a somewhat different shape. In general, all the flame profiles were similar to Fig. 12, but with different center positions and widths.

A typical profile of the rms fluctuation in the Rayleigh signal is shown in Fig. 13 for a position 6 mm downstream from the flame holder. The fluctuations decrease to zero outside the flame zone, as expected.

The other fluctuation profiles are fairly similar.

The correlation of the center of the flame density profiles with the center of the flame fluctuation profiles is shown in Fig. 14. This correlation is quite good, and it appears that the two centers coincide quite well. The correlation of the width of the flame density profiles with the width of the flame fluctuation profiles, shown in Fig. 15, is not so good. The flame width was taken as defined by Eq. 3 and the half peak intensity width was used for the width of the flame fluctuation profile. We believe that the scatter is due to the previously discussed errors in the data, which are exaggerated by the differencing required to obtain the widths. Within these errors, the two widths appear comparable.

The position of the flame front as determined by a series of transverse profile measurements at various axial locations is shown in Fig. 16. The mean location is taken from the center of the fluctuation profiles, and the "error bars" indicate the half-intensity width of the fluctuation profiles. Also shown on the figure is the location of the flame in the absence of the wake generating rod. The flame moves substantially closer to the rod, as would be expected due to the decreased velocity in the wake region. There may also be an increase in the flame propagation velocity due to the increased mixing in the wake vortices; however, detailed velocity measurements would be necessary to determine this effect.

Measurements of the mean and rms velocities in the wake of the rod were made using a hot film anemometer probe, in the absence of the flame. The profiles agreed with the measurements of Kovásznay<sup>(14)</sup>, and the width of the fluctuation region, based on the 5% normalized rms level, is shown in Fig. 16. The maximum rms fluctuations were about 12%. It is immediately obvious that the width of the flame region is much less than the width of

the wake. However, the rms fluctuations in velocity in the wake of the cylinders were comparable to the rms fluctuations in Rayleigh scattering through the flame. Further, there are fluctuations in the flame location close to the flame holder where there is no disturbance of the flow by the wake, at least in the case where the flame is absent.

In the presence of the flame the streamlines upstream of the flame are curved outward from the center of the channel, due to the partial blocking of the flow by the density decrease associated with the flame. As a result the wake of the rod will also be curved outward. Since the presence of the flame front affects the entire flow field in the region upstream of the front, it is reasonable that the fluctuating flame will cause a fluctuating perturbation of the flow field. This could be responsible for the fluctuations in the flame front in the region close to the flame holder where the flow is not directly affected by the wake of the cylinder.

The width of the fluctuating flame region, indicated by the bars in Fig. 16, is shown in Fig. 17 plotted against the transverse flame positions. There appears to be nearly linear increase in width in the region near the flame holder, a leveling off directly above the rod, followed by a sharp increase to about 1.5 mm, after which it remained fairly constant.

A study of plane oscillating flame fronts has previously been reported by Peterson and Emmons<sup>(15)</sup>, where a flame holder was oscillated transverse to the flow and the shape of the flame front was recorded. At low frequencies the oscillations grow slowly in amplitude as one progresses along the flame front, away from the origin, while at higher frequencies the oscillations are damped. Their measurements are in reasonable agreement with a theoretical description due to Markstein<sup>(16)</sup>. These results predict a very moderate decay of the 22 Hz oscillations found in the present measurements. It is not clear what bearing this has on the present experiment, except in the region furthest from the flame holder

where the flow perturbation due to the wake should be small. In this region the oscillations are probably generated upstream in the stronger wake region and the flame structure should have an oscillating shape. However, in the region near the flame holder the oscillations should be of different character, perhaps due to perturbations in the flow velocity as discussed earlier. The wake region itself has a strong vortex structure which will directly affect the flame propagation.

#### SUMMARY

An experimental apparatus and technique for studying the effect of flow fluctuations and turbulence on plane flame fronts has been developed. The diagnostic techniques consist of Rayleigh scattering for time resolved density measurements and laser Doppler velocimetry for velocity measurements.

When a plane flame front, originating at a small wire or rod, is created in an open methane/air jet, there are appreciable fluctuations in the flame front densities at all positions along the flame even though, in the absence of the flame front, the flow is quite steady in the central core. The large scale turbulent eddies in the mixing region of the jet and the ambient air cause the flame to fluctuate considerably in this region and it appears as though these fluctuations are able to perturb the flame front upstream in the central core.

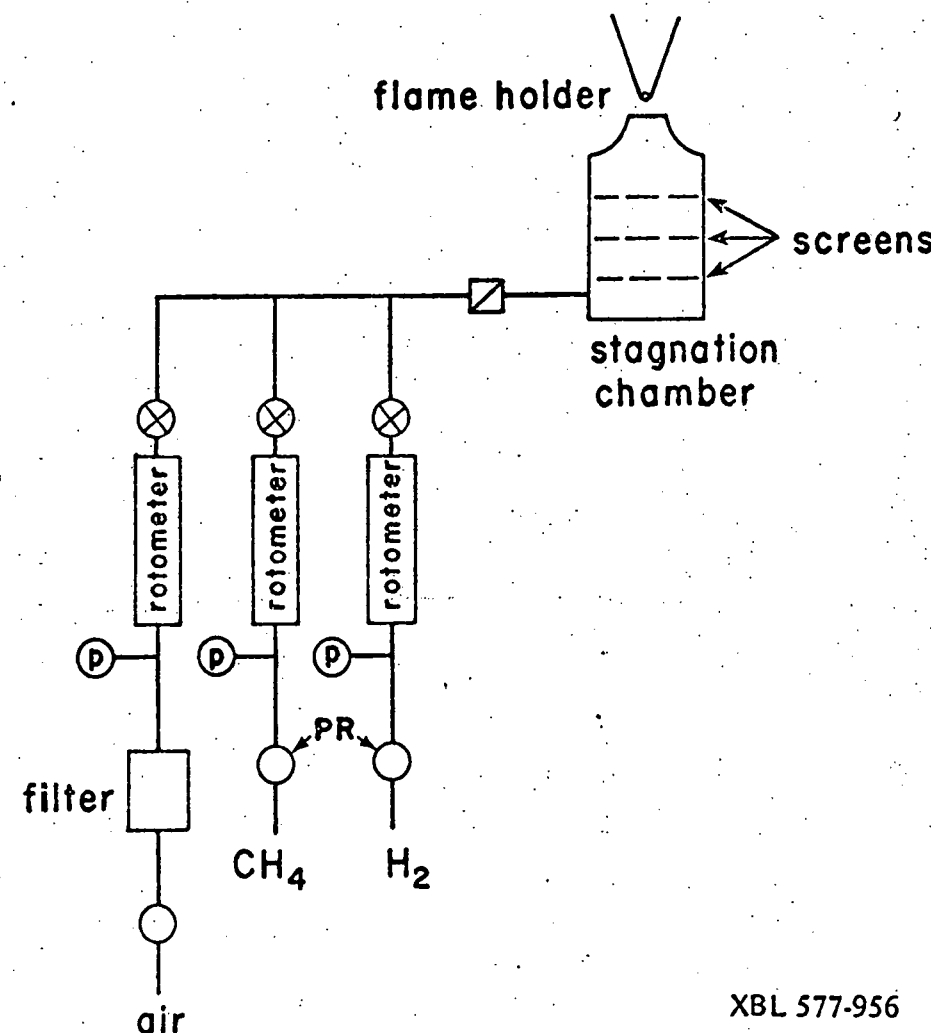
By enclosing the flow in a square channel with pyrex glass walls, a steady plane flame front could be generated. A preliminary study of the interactions of the flame front with the vortices shed from a cylinder

was carried out. Fluctuations in the flame front were found both upstream and downstream of the wake region of the cylinder. In the wake regions, the width of the fluctuating flame front was small compared to the scale of the vortices generated by the cylinder, although the rms values of wake velocity fluctuations and flame density fluctuations were comparable. As in the open jet measurements, it appeared as though the flame front fluctuations in the wake region were able to perturb the flame front upstream in the flow region which was undisturbed by the wake (at least in the absence of a flame).

It appears that motion of the flame front will perturb the entire flow field, so that the flame position and the direction and velocity of the flow before the flame front are coupled. In fact, it is well known that the laminar sheet flame fronts stabilized on a rod create a wedge-type flow around the flame, considerably perturbing the flow upstream of the flame. It then follows that if a region of the flame front is fluctuating, then it will cause fluctuations in the upstream flow. This may be a mechanism which is capable of explaining the upstream flame fluctuations observed both in the open jet flow and in the channel flow perturbed by the wake of a cylinder.

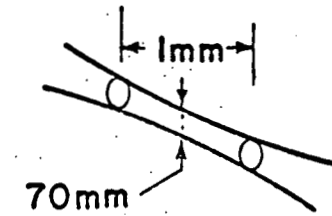
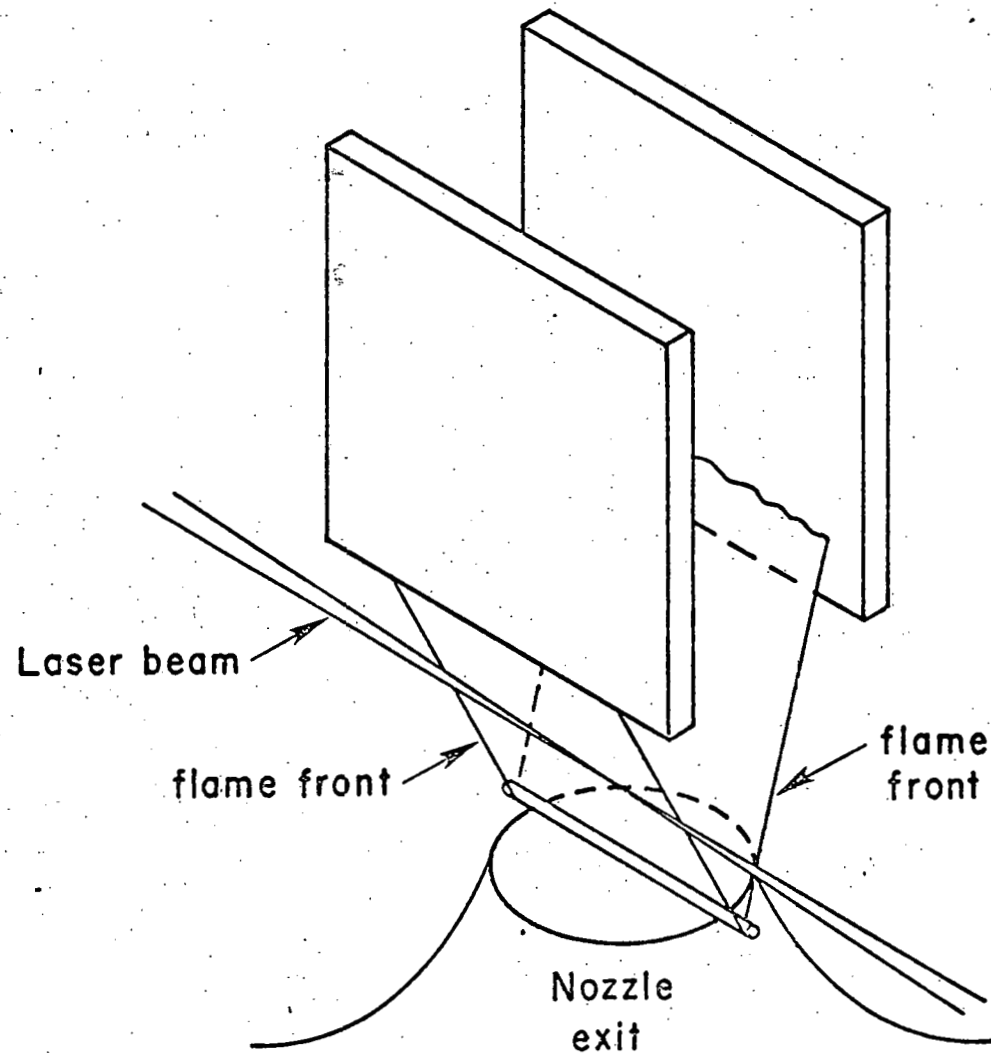
REFERENCES

1. Williams, F. A., Combustion Theory, Addison-Wesley, London, 1965.
2. Beer, J. M. and Chigier, N. A., Combustion Aerodynamics, Halsted Press, New York, 1972, p. 60.
3. Schefer, R. A. and Sawyer, R. F., Sixteenth Symposium (International) on Combustion, The Combustion Institute, (to be published).
4. Pratt, D. T., Fifteenth Symposium (International) on Combustion, 1339, The Combustion Institute, 1975.
5. Laufer, J., Annual Review of Fluid Mechanics, 7, 1975, pp. 307-326.
6. Lewis, B. and von Elbe, G., Combustion, Flames, and Explosions in Gases, Academic Press, New York, 1961.
7. Robben, F., "Comparison of Density and Temperature Measurement Using Raman Scattering and Rayleigh Scattering," presented at Workshop on Combustion Measurements in Jet Propulsion Systems, Lafayette, Ind., May 22-23, 1975.
8. Chigier, N. A., "Combustion Diagnostics by Laser Velocimetry," 14th Aerospace Sciences Meeting, paper 76-32, Jan. 1976, Washington, D.C.
9. Rudd, M. J., J. of Physics, 2, 1969.
10. Andrews, G. E. and Bradley, D., Comb. Flame, 19, 275, 1972.
11. Smith, K. O. and Gouldin, F. C., "Experimental Investigation of Flow Turbulence Effects on Premixed Methane-air Flames," AIAA 15th Aerospace Sciences meeting, paper 77-183, Los Angeles, CA, Jan. 24-26, 1977.
12. Fristrom, R. M. and Westenberg, A. A., Flame Structure, McGraw-Hill, New York, 1965.
13. Stephenson, D. A., private communication, G. M. Corp. Laboratories, Warren, Mich.
14. Kovásznay, L. S. G., Proc. Roy. Soc., A. 198, 174-190, 1949.
15. Peterson, R. E., Emmons, H. W., Phys. of Fluids, 4, no. 4, p. 456, 1961.
16. Markstein, G. H. ed., "Non-Steady Flame Propagation," Macmillan Co. New York, 1964.



XBL 577-956

FIGURE 1. Experimental Apparatus



Details of Raleigh  
Measuring Volumen

XBL 577-957

FIGURE 2. Wire Stabilized Flame

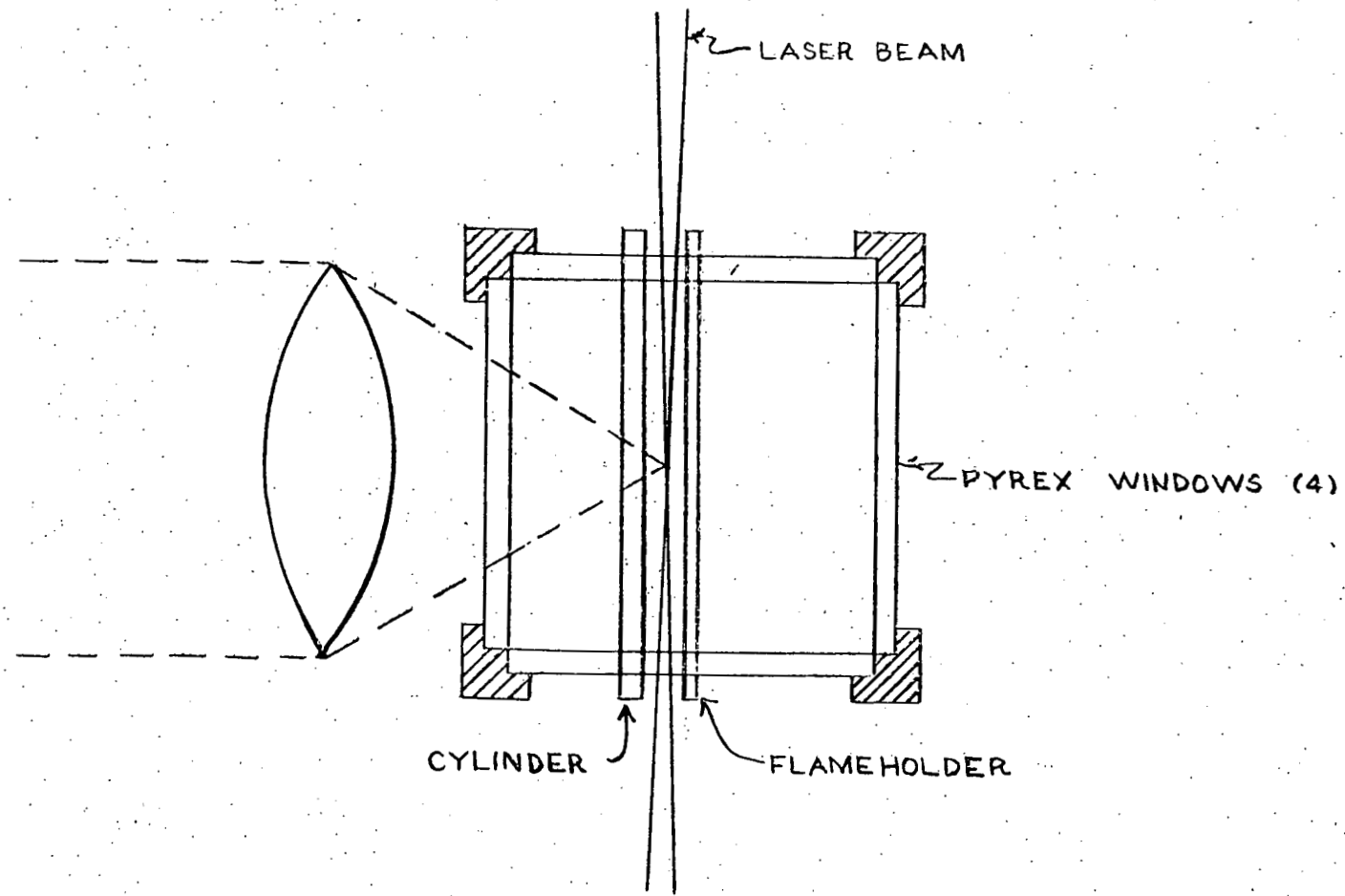


Figure 3. Top view of square channel

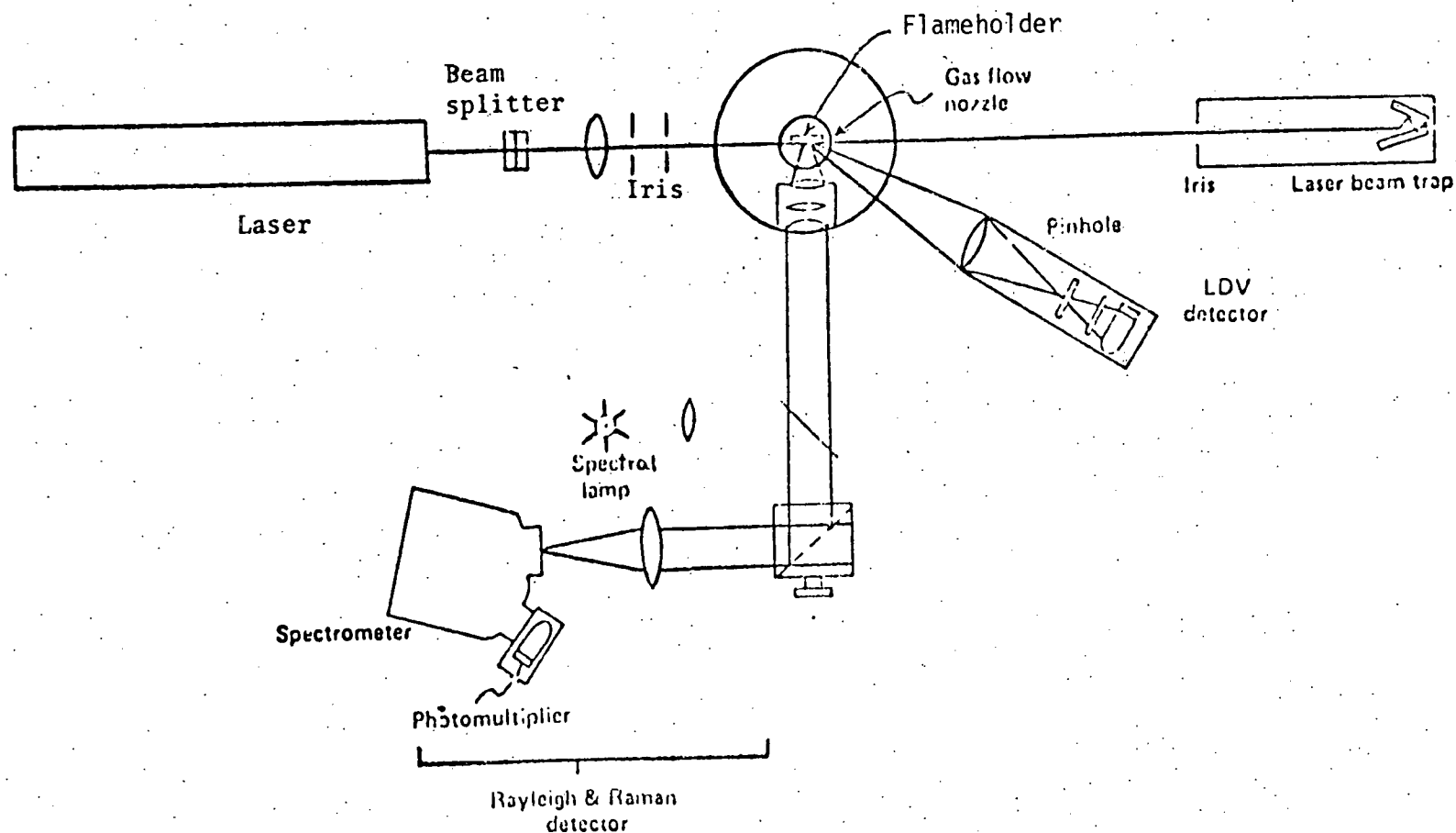
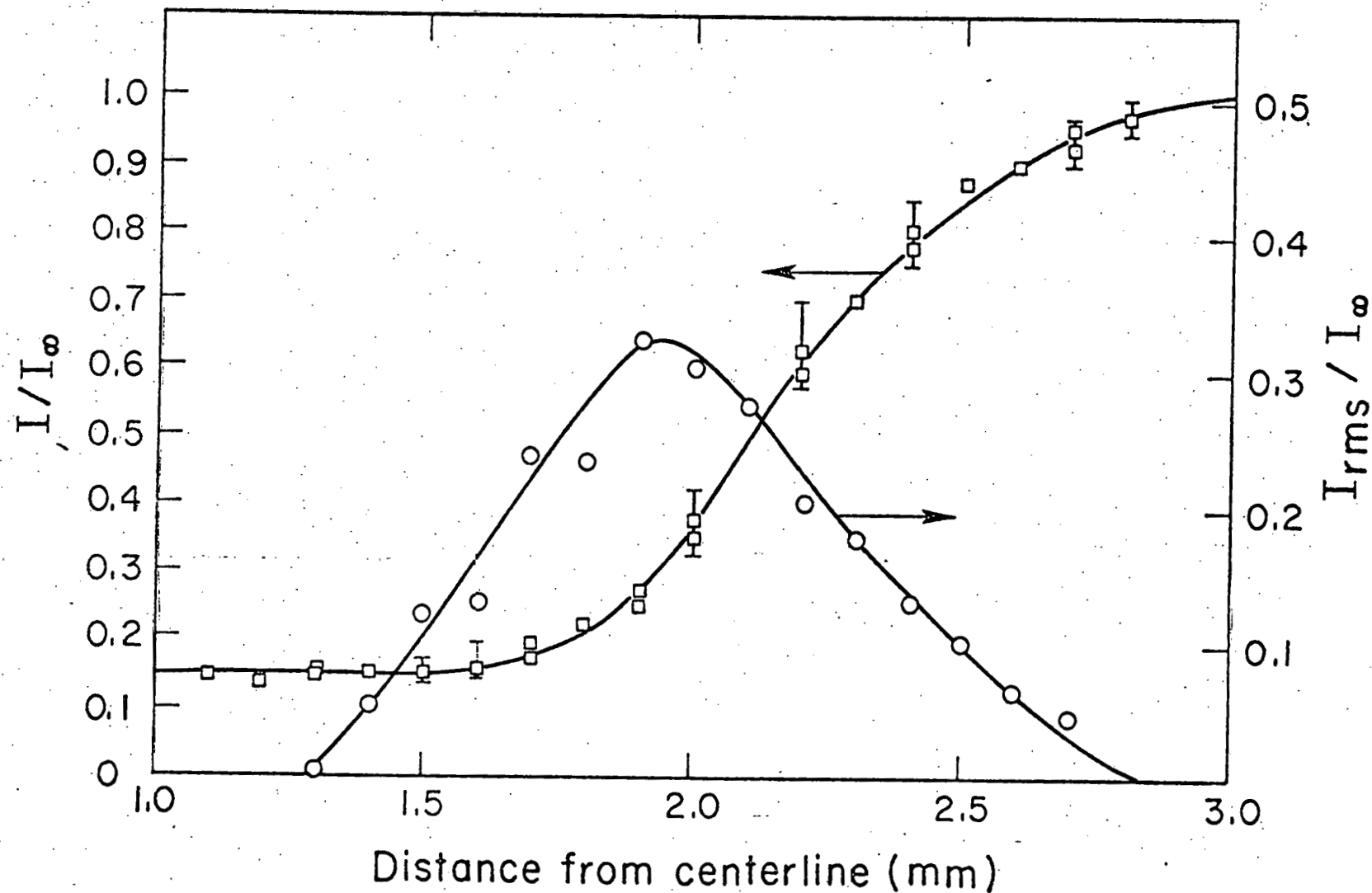


Figure 4  
Rayleigh and LDV System



XBL 577-958

FIGURE 5. Variation of normalized Rayleigh scattering intensity and RMS fluctuations with distance from centerline. Traverse at 3 mm above wire.

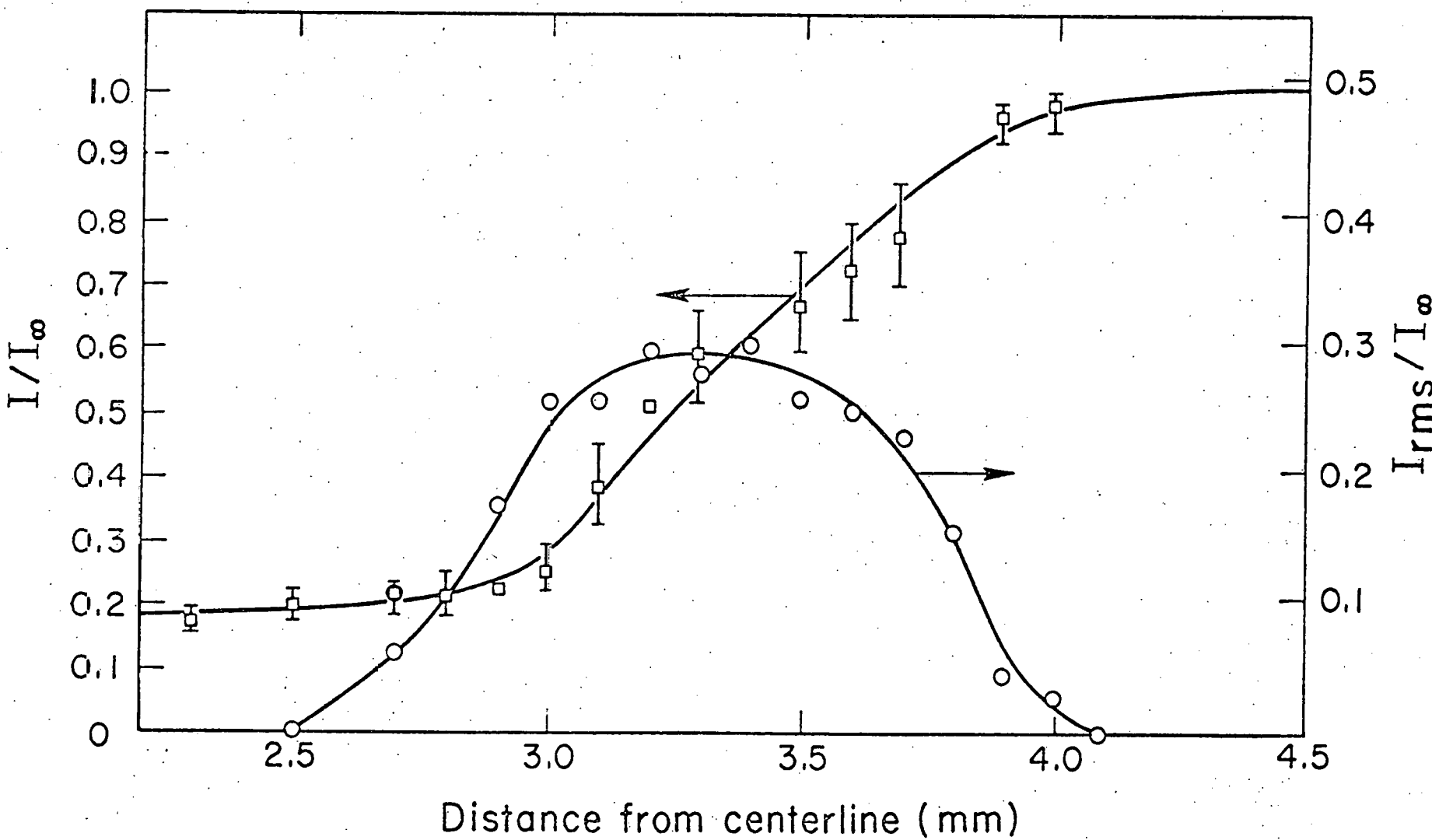


FIGURE 6. Variation of normalized Rayleigh scattering intensity and RMS fluctuations with distance from centerline. Traverse at 6 mm above wire.

XBL 577-959

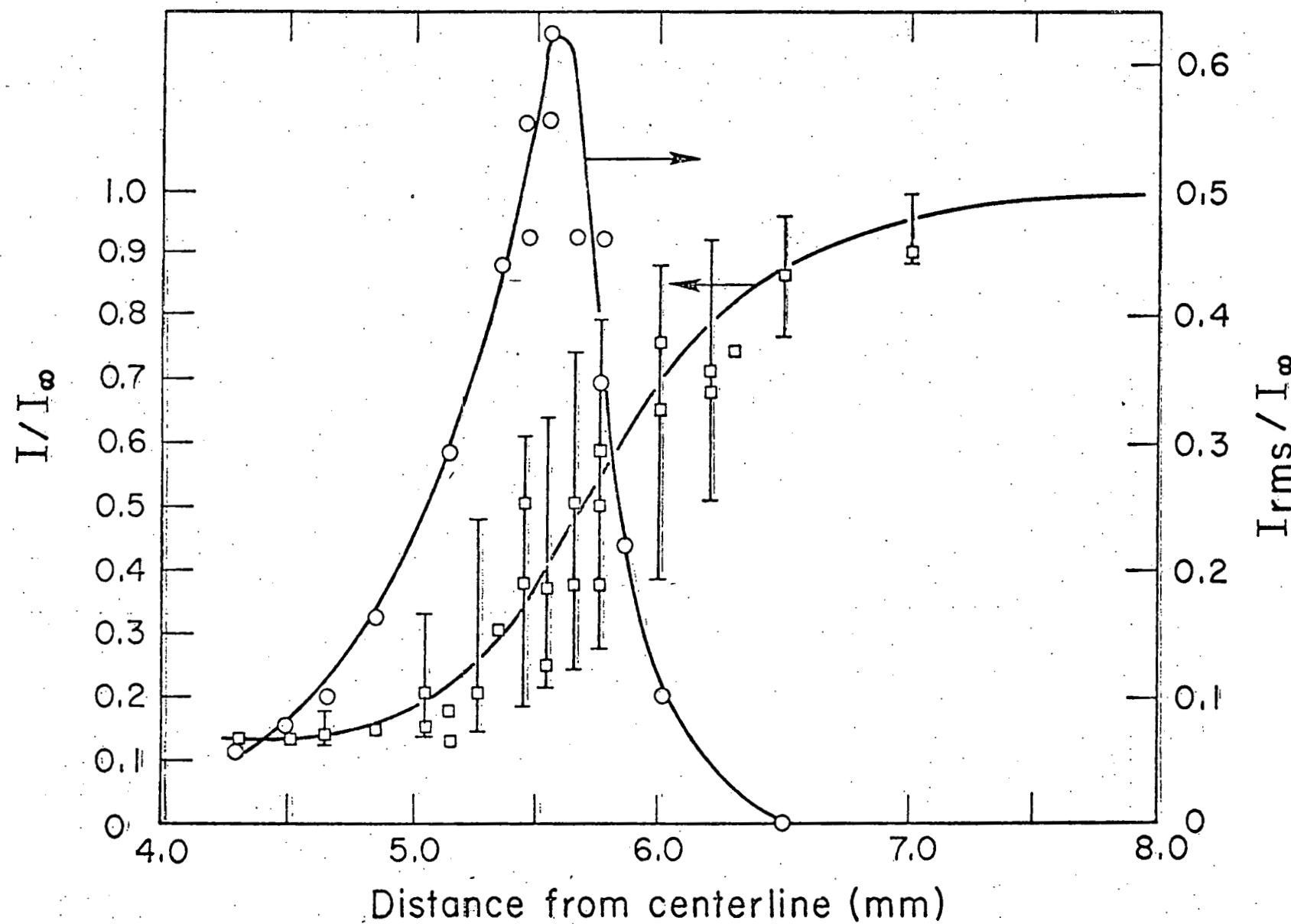


FIGURE 7. Variation of normalized Rayleigh scattering intensity and RMS fluctuations with distance from centerline. Traverse at 12 mm above wire.

XBL 577-962

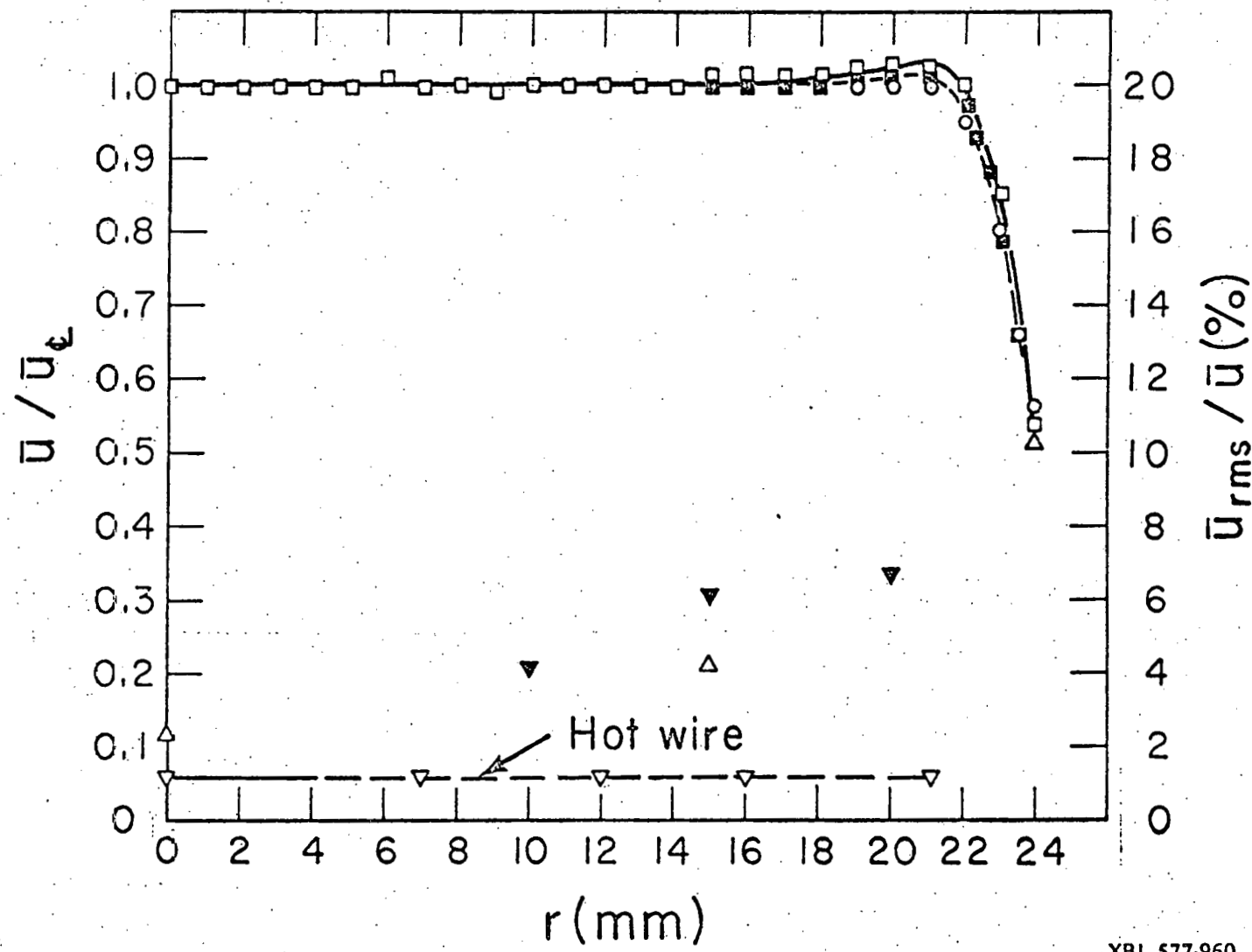
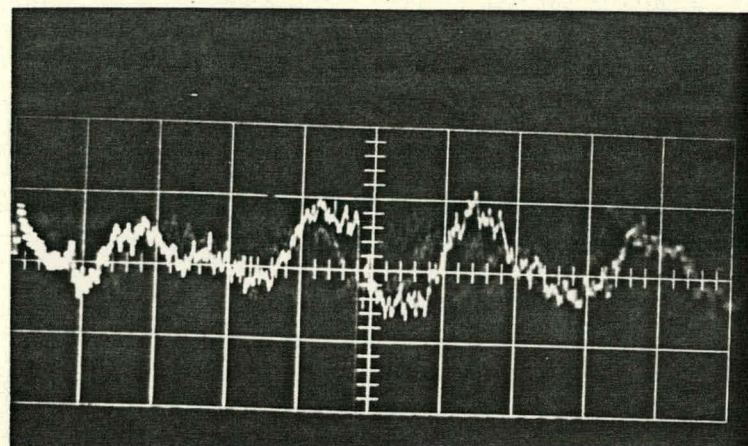
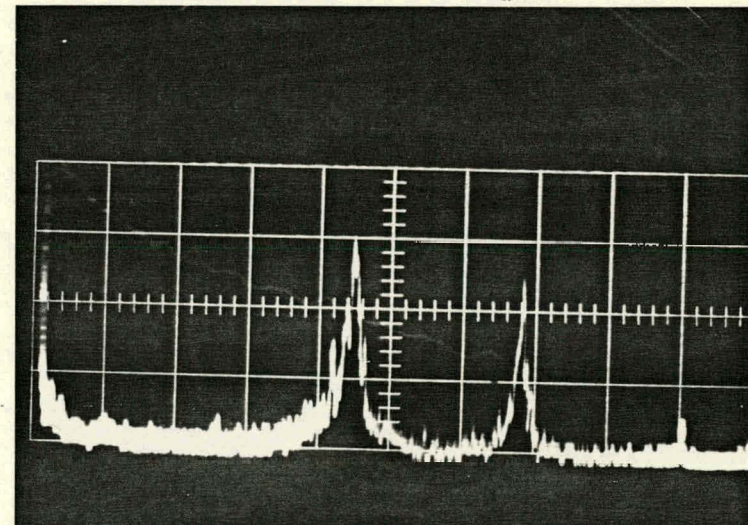


FIGURE 8. Velocity profiles and rms fluctuations above the nozzle without combustion. Mean velocity:  
 $\square$  -  $z = 3$  mm,  $\blacksquare$  -  $z = 6$  mm,  $\circ$  -  $z = 12$  mm;  
 RMS fluctuations:  $\nabla$  -  $z' = 3$  mm,  $\Delta$  -  $z = 6$  mm,  
 $\blacktriangledown$  -  $z = 12$  mm.

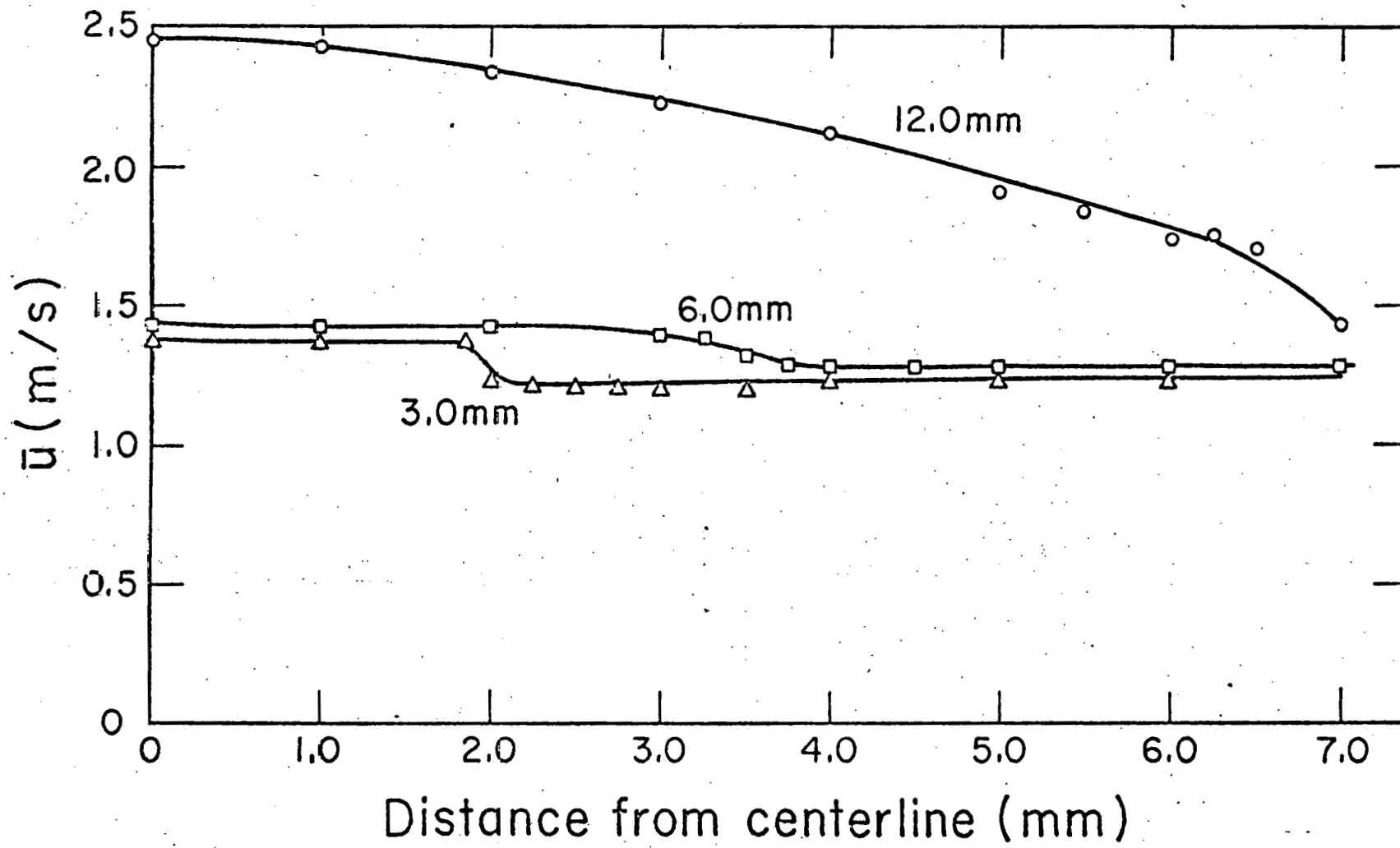
XBL 577-960



Oscilloscope trace of Rayleigh signal 6 mm from nozzle exit and 3.5 mm from centerline (5 ms/cm sweep rate).



Spectrum of Rayleigh signal.  
(200 Hz full scale).



XBL 577-961

FIGURE 10. Variation of velocity with distance from centerline  
Traverses at 3 mm, 6 mm and 12 mm downstream from  
nozzle exit.

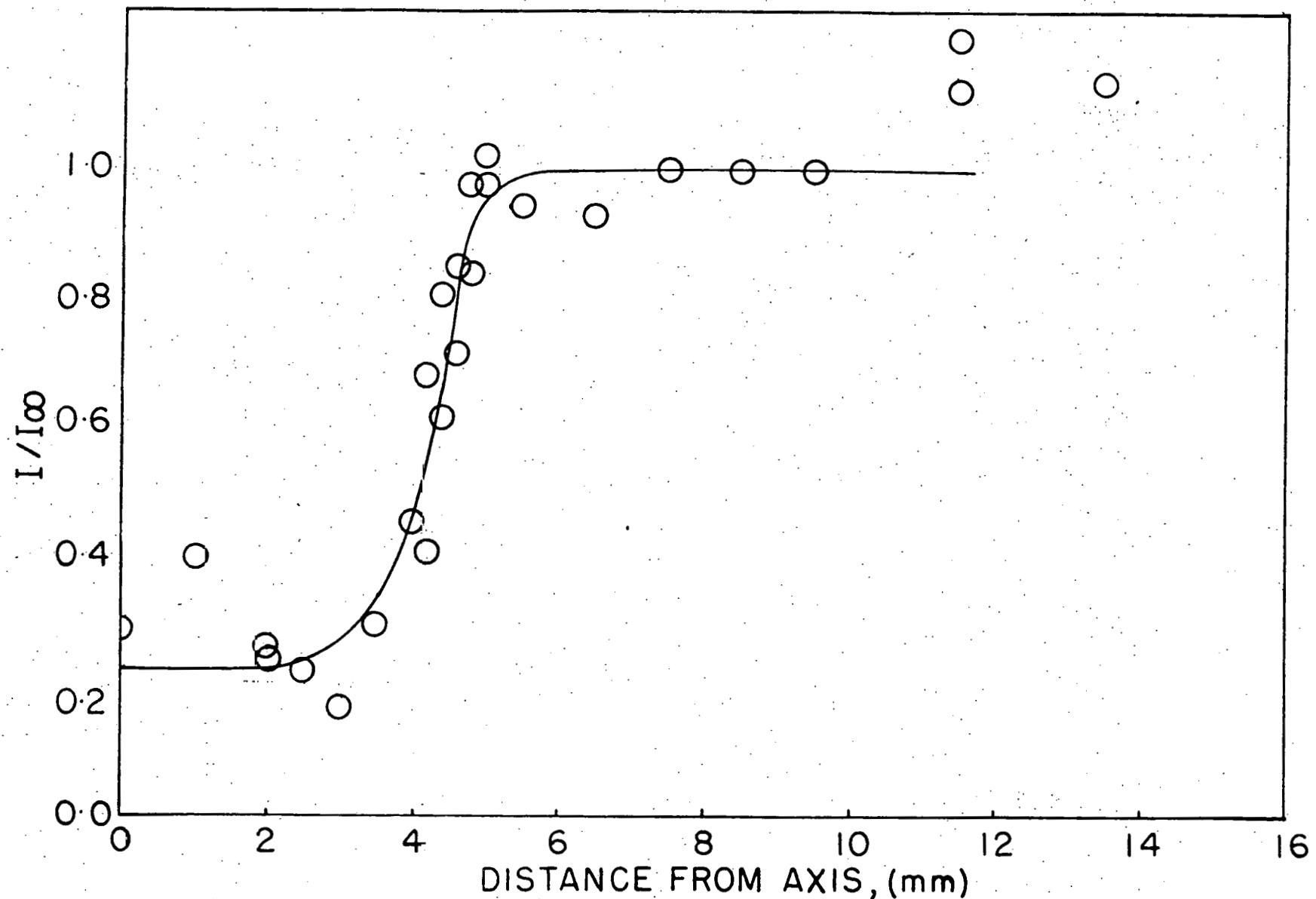


Figure 11. Variation of normalized Rayleigh scattering intensity with distance from centerline at 5 mm above flameholder for undisturbed flame.

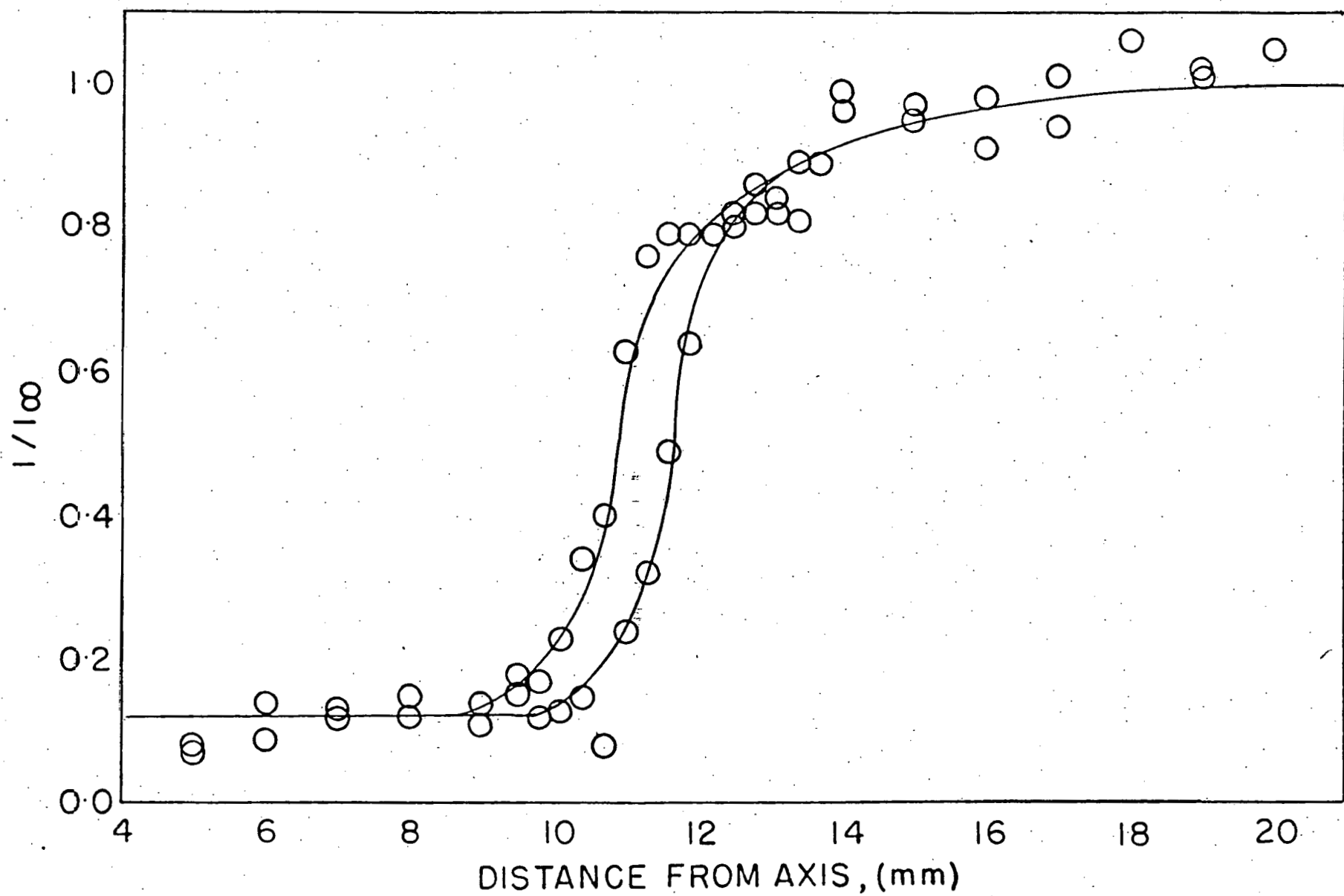


Figure 12. Variation of normalized Rayleigh scattering intensity with distance from centerline at 12.5 mm above flameholder for flame disturbed by the wake behind cylinder.

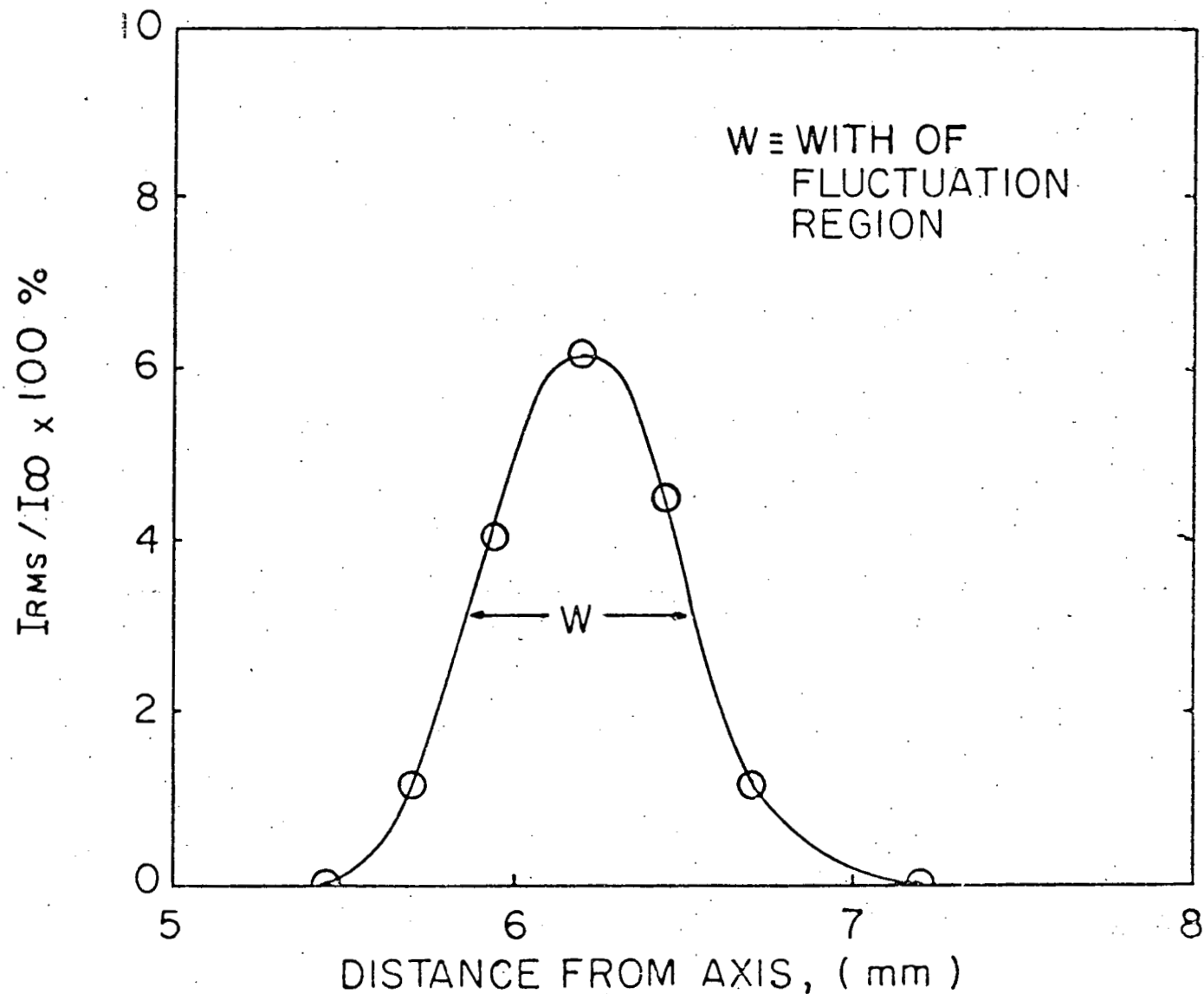


Figure 13. RMS fluctuations with distance from centerline at 6 mm above flameholder.

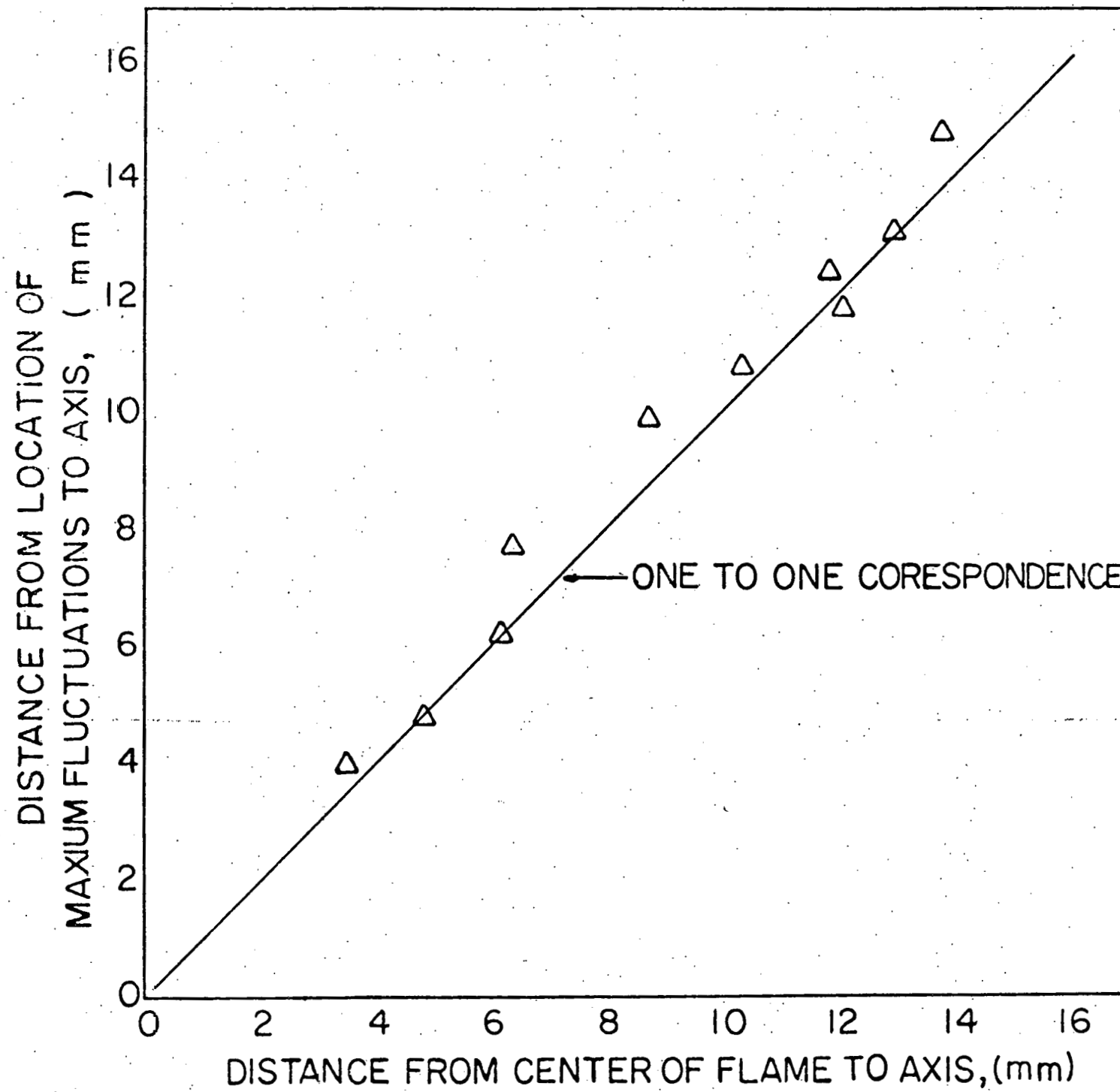


Figure 14. Correlation of flame location with location of maximum RMS fluctuation.

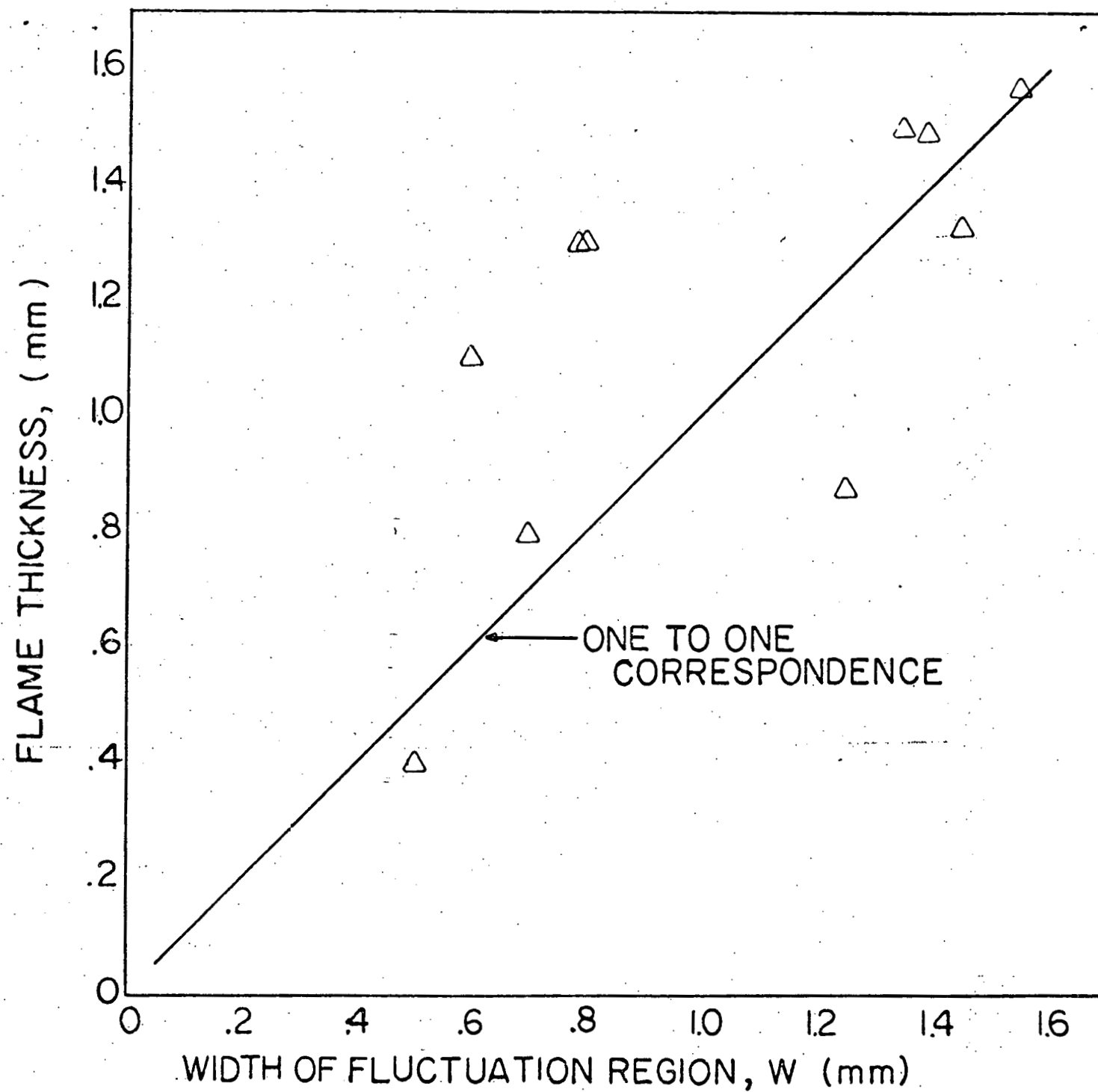


Figure 15. Correlation of flame thickness with width of RMS fluctuations.

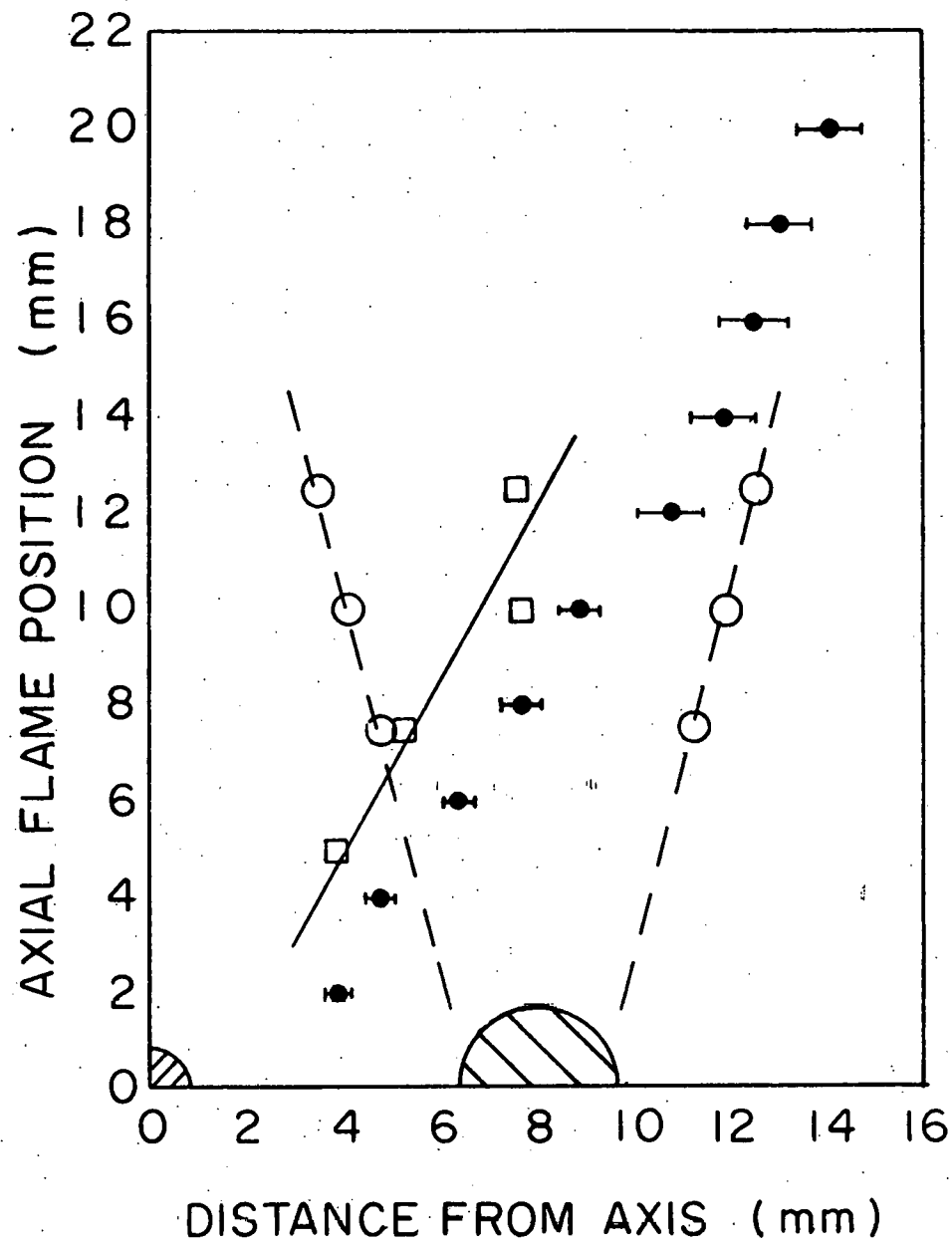


Figure 16. Flame location

□ - for undisturbed flame

● - for flame disturbed by the wake  
behind a cylinder

○ - boundary of the wake of the cylinder

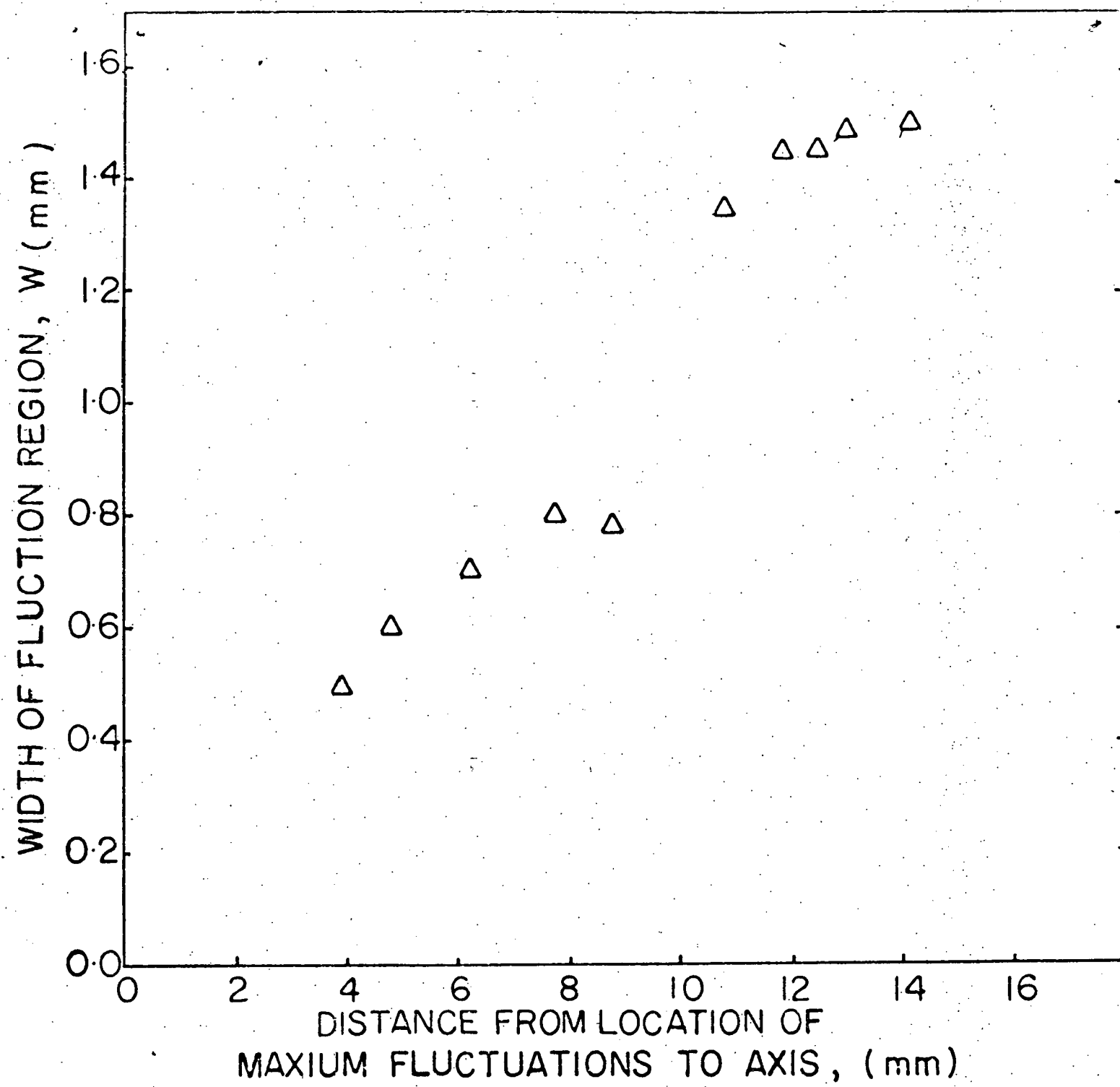


Figure 17. Width of RMS fluctuations with distance from centerline.